ORGANOMETALLICS

Article

pubs.acs.org/Organometallics

Nickel(II) Complexes Containing Bidentate Diarylamido Phosphine Chelates: Kumada Couplings Kinetically Preferred to β-Hydrogen Elimination

Ming-Tsz Chen,[†,§] Wei-Ying Lee,[†,§] Tzung-Ling Tsai,[†] and Lan-Chang Liang*[,†,‡]

[†]Department of Chemistry and Center for Nanoscience & Nanotechnology, National Sun Yat-sen University, 70 Lien-Hai Road, Kaohsiung 80424, Taiwan

[‡]Department of Medicinal and Applied Chemistry, Kaohsiung Medical University, Kaohsiung 80708, Taiwan

Supporting Information

ABSTRACT: A series of divalent nickel complexes containing diarylamido phosphine ligands of the type $(o\text{-}ArNC_6H_4PR_2)^-$ (**1a**, Ar = 2,6-$C_6H_3Me_2$, R = Ph; **1b**, Ar = 2,6-$C_6H_3iPr_2$, R = Ph; **1c**, Ar = 2,6-$C_6H_3Me_2$, R = *i*Pr; **1d**, Ar = 2,6-$C_6H_3iPr_2$, R = *i*Pr) have been prepared and structurally characterized. The dimeric nickel chloride derivatives $\{[\mathbf{1b-d}]Ni(\mu\text{-}Cl)\}_2$ (**2b–d**) were isolated as brick red microcrystals in high yields from the reactions of $NiCl_2(DME)$ with either $Li[\mathbf{1b-d}](solv)_x$ or H[**1b–d**] in the presence of NEt_3. Similar reactions employing $[\mathbf{1a}]^-$, however, generated homoleptic Ni[**1a**]$_2$ (**3a**) as paramagnetic, dark red prisms in high yield. Addition of trimethylphosphine to red solutions of **2b,c** in THF at room temperature afforded emerald crystals of [**1b,c**]NiCl(PMe_3) (**4b,c**). Interestingly, solution NMR spectroscopic and X-ray crystallographic data of these PMe_3 adducts reveal the exclusive formation of *cis*-**4b** and *trans*-**4c**, as defined by the mutual orientation of the two phosphorus donors incorporated. Metathetical reactions of **4b,c** with RMgCl (R = Me, CH_2SiMe_3, Ph) in THF at −35 °C produced high yields of red or brownish red crystalline [**1b,c**]NiR(PMe_3) (R = Me (**5b,c**), CH_2SiMe_3 (**6b,c**), Ph (**7b,c**)). Analogous reactions of **4c** with EtMgCl or *n*BuMgCl, however, led instead to the isolation of the hydrido species [**1c**]NiH(PMe_3) (**8c**) in quantitative yield. Solution NMR data of the methyl complexes **5b,c** indicate the presence of both cis and trans isomers; the major component of **5b** is cis whereas that of **5c** is trans. In contrast, complexes **6b,c**, **7b,c**, and **8c** all exist exclusively in the trans form. The chloro complexes **2b–d** are all active catalyst precursors for Kumada couplings under mild conditions. In particular, this catalysis is compatible with alkyl nucleophiles that contain β-hydrogen atoms, even in reactions with chlorobenzene. The X-ray structures of **2d**, **3a**, **4c**, **5c**, **6b,c**, **7c**, and **8c** are presented.

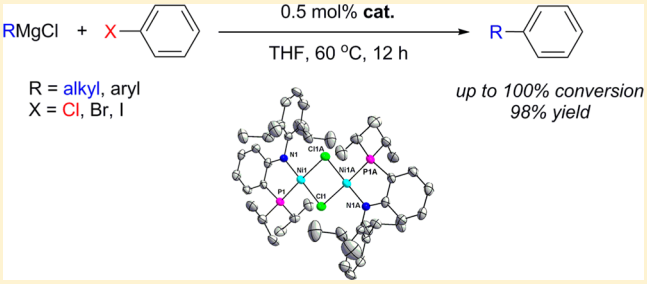

INTRODUCTION

Tremendous efforts have been made in the past decades by synthetic chemists to find appropriate methods to facilitate C–C bond-forming reactions.[1,2] Transition-metal-catalyzed cross-coupling reactions of Grignard reagents with (pseudo)-halogenated hydrocarbon electrophiles, generally referred to as Kumada couplings, have proven to be some of the most powerful and valuable protocols for organic syntheses.[3−5] Though widely employed, cross-coupling reactions, broadly defined, often suffer from incompatibilities with alkyl building blocks that contain β-hydrogen atoms, for which β-hydrogen elimination is usually a kinetically more accessible process.[6,7] Moreover, the hydrido complexes thus produced are generally more thermodynamically stable than their corresponding metal–alkyl precursors, in turn giving unwanted hydro-dehalogenated instead of the desired cross-coupled products.

Several examples are now known to facilitate Kumada couplings compatible with β-hydrogen-containing alkyl building blocks.[8−16] Our interests in exploratory chemistry employing diarylamido phosphine complexes[17−28] have led us to discover that nickel chloride complexes of PNP (Figure 1) are active catalyst precursors for Kumada coupling reactions, including those involving β-hydrogen-containing alkyls.[29] The success of this catalysis is ascribed, in part, to the unusual inherent nature of organonickel complexes of PNP, wherein β-hydrogen elimination is a thermodynamically uphill process,[30] as corroborated by its reverse reactions in view of the principle of microscopic reverse: i.e., insertion reactivity of [PNP]NiH with $H_2C{=}CHR$ to give [PNP]$NiCH_2CH_2R$ that is markedly thermally stable even at elevated temperatures. In this particular study, the nondissociative characteristics of the phosphorus donors incorporated are believed to be crucial.[31] Upon the inclusion of an ethylene tethered amino donor that is characteristic of having

Special Issue: Catalytic and Organometallic Chemistry of Earth-Abundant Metals

Received: June 15, 2014

   dx.doi.org/10.1021/om5006353 | *Organometallics* XXXX, XXX, XXX–XXX

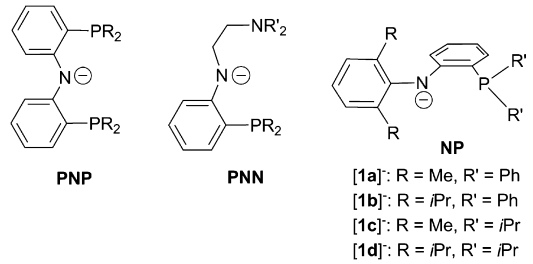

Figure 1. Representative examples of *o*-phenylene-derived amido phosphine ligands.

higher hemilability, the PNN complexes of nickel alkyls also resist β-elimination at elevated temperatures and facilitate effectively catalytic Kumada couplings compatible with β-hydrogen-containing alkyl building blocks.[32] A notable discrepancy in Kumada activities between PNP- and PNN-ligated complexes concerns the comparatively higher reactivity and selectivity of the latter.[32] In line with these intriguing results and the fundamental concepts concerning dynamic κ^2 and κ^3 coordination modes of PNN, we became interested in exploratory chemistry of nickel complexes containing bidentate NP chelates,[33] in particular their compatibility with catalytic Kumada couplings involving β-hydrogen-containing alkyls. In this contribution, we show evidence that β-hydrogen elimination does occur in this particular system for thermodynamic reasons, but complexes derived herein are yet superior catalysts for β-hydrogen-containing alkyl Grignard reagents to couple with aryl halides, including inherently more challenging chloro electrophiles. We describe herein the synthesis and structural characterization of nickel complexes supported by a series of NP ligands $[\mathbf{1a}-\mathbf{d}]^-$ and their reactivity study with respect to Kumada-type catalysis. Factors to determine thermodynamically favored stereochemistry that these four-coordinate complexes prefer, i.e., cis versus trans isomers, are also discussed.

RESULTS AND DISCUSSION

Equation 1 illustrates the synthetic strategies to prepare nickel chloride complexes **2**. Compounds **2c**,**d** were both prepared in a manner similar to that established previously for **2b**[33] as brick red microcrystals in high yields by treating $NiCl_2(DME)$[34] with either $Li[\mathbf{1c}-\mathbf{d}](solv)_2$ (solv = THF for **1c**, 0.5 DME for **1d**)[35] or $H[\mathbf{1c}-\mathbf{d}]$[35] in the presence of NEt_3. The solution NMR data of these chloride complexes are all consistent with a structure having a reflection symmetry. For instance, the ^1H NMR spectrum of **2c** in C_6D_6 reveals a multiplet resonance at 1.61 ppm for the C*H*Me_2 groups bound to the phosphorus donor and a singlet at 2.60 ppm for the ortho N-aryl methyl groups. The phosphorus donor in these nickel chloride complexes generally resonates significantly downfield in comparison to those of their corresponding protio or lithio precursors: e.g., 62.6 ppm for **2c** versus −17.4 ppm for $H[\mathbf{1c}]$[35] and −7.9 ppm for $[\mathbf{1c}]Li(THF)_2$.[35] Compounds bearing P-alkyl substituents, including protio, lithium, and nickel derivatives, typically give rise to relatively downfield ^{31}P signals in comparison with their P-arylated counterparts: e.g., 62.6 ppm for **2c** and 60.2 ppm for **2d** versus 32.5 ppm for **2b**.[33] Selected NMR data are summarized in Table 1.

$$H[\mathbf{1b}-\mathbf{d}] \xrightarrow{NiCl_2(DME),\ NEt_3} \underset{\mathbf{2b}-\mathbf{d}}{\{[\mathbf{1b}-\mathbf{d}]Ni(\mu\text{-}Cl)\}_2} \xleftarrow{NiCl_2(DME)} [\mathbf{1b}-\mathbf{d}]Li(solv)_2 \quad (1)$$

Table 1. Selected NMR Spectroscopic Data[a]

compd	δ_P^{NP}	δ_P^{PMe3}	$^2J_{PP}$	$\delta_{H\alpha}$	$^3J_{PH\alpha}$	$\delta_{C\alpha}$	$^2J_{PC\alpha}$
$H[\mathbf{1a}]$[b]	−19.3						
$[\mathbf{1a}]Li(THF)_2$[c]	−13.7						
$\{[\mathbf{1a}]Ni(\mu\text{-}Cl)\}_2$ (**2a**)	32.0[d]						
$H[\mathbf{1b}]$[e]	−20.1						
$[\mathbf{1b}]Li(THF)_2$[e]	−12.0						
$\{[\mathbf{1b}]Ni(\mu\text{-}Cl)\}_2$ (**2b**)[c]	32.5						
$[\mathbf{1b}]NiCl(PMe_3)$ (**4b**)[c]	47.3	−17.0	88				
$[\mathbf{1b}]NiMe(PMe_3)$ (**5b**)[c,f]	35.6	−7.5	25	−0.12	4.0, 7.5	11.1	39, 59
$[\mathbf{1b}]NiMe(PMe_3)$ (**5b**)[c,g]	39.0	−18.0	301	−0.42	7.5, 12.0	N/A[h]	N/A[h]
$[\mathbf{1b}]NiCH_2SiMe_3(PMe_3)$ (**6b**)	34.4	−22.5	318	−0.70	N/A[i]	−13.4	18, 25
$[\mathbf{1b}]NiPh(PMe_3)$ (**7b**)[c]	33.0	−22.3	288			151.9	34, 39
$H[\mathbf{1c}]$[j]	−17.4						
$[\mathbf{1c}]Li(THF)_2$[j]	−7.9						
$\{[\mathbf{1c}]Ni(\mu\text{-}Cl)\}_2$ (**2c**)	62.6						
$[\mathbf{1c}]NiCl(PMe_3)$ (**4c**)	51.1	−24.2	314				
$[\mathbf{1c}]NiMe(PMe_3)$ (**5c**)[f]	45.5	−20.0	296	−0.69	7.0, 13.0	−18.5	23, 34
$[\mathbf{1c}]NiMe(PMe_3)$ (**5c**)[g]	47.7	−9.1	22	−0.42	3.5, 7.5	N/A[h]	N/A[h]
$[\mathbf{1c}]NiCH_2SiMe_3(PMe_3)$ (**6c**)	42.9	−26.3	305	−0.93	10.5, 15.5	−18.9	17, 30
$[\mathbf{1c}]NiPh(PMe_3)$ (**7c**)	40.6	−24.3	278			150.9	34, 41
$[\mathbf{1c}]NiH(PMe_3)$ (**8c**)	63.3	−19.9	263	−20.2[k]	72.5, 82.0[k]		
$H[\mathbf{1d}]$[j]	−17.2						
$[\mathbf{1d}]Li(DME)$[j]	−7.3						
$\{[\mathbf{1d}]Ni(\mu\text{-}Cl)\}_2$ (**2d**)	60.2						

[a]Unless otherwise noted, all spectra were recorded in C_6D_6 at room temperature. Chemical shifts are given in ppm and coupling constants in Hz. [b]Data selected from ref 36. [c]Data selected from ref 33. [d]Tentative assignment (see context for details), recorded in THF. [e]Data selected from ref 37. [f]Data summarized correspond to the major component of the two geometric isomers produced. [g]Data summarized correspond to the minor component of the two geometric isomers produced. [h]Signal intensities are too low to confirm. [i]Too broad to determine. [j]Data selected from ref 35. [k]Chemical shift δ_H (instead of $\delta_{H\alpha}$) and coupling constants $^2J_{PH}$ (instead of $^3J_{PH\alpha}$) correspond to the nickel-bound hydride ligand, not H_α.

dx.doi.org/10.1021/om5006353 | *Organometallics* XXXX, XXX, XXX−XXX

Attempts to grow crystals of **2b,c** for X-ray diffraction analysis were not successful. X-ray-quality crystals of **2d**, however, were obtained by layering pentane on a concentrated diethyl ether solution at −35 °C. As deduced in the previous report,[33] complexes **2** exist as chloride-bridged dimers in the solid state. Figure 2 depicts the X-ray structure of **2d**. The

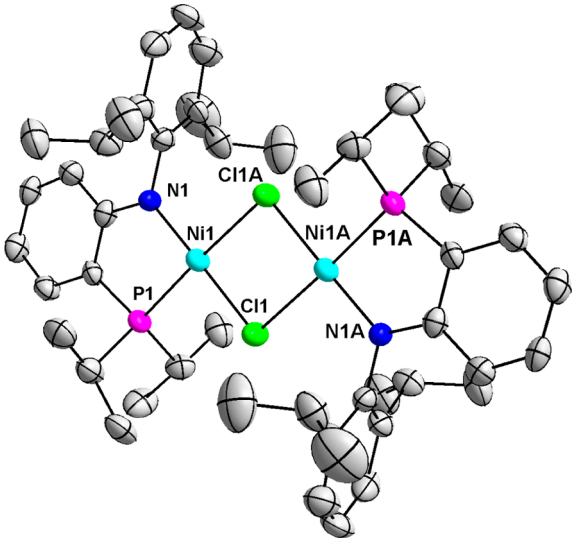

Figure 2. Molecular structure of **2d** with thermal ellipsoids drawn at the 35% probability level. Selected bond distances (Å) and angles (deg): Ni1−N1, 1.881(7); Ni1−P1, 2.131(2); Ni1−Cl1, 2.196(3); Ni1−Cl1A, 2.267(2); N1−Ni1−P1, 86.1(2); N1−Ni1−Cl1, 178.0(2); P1−Ni1−Cl1, 92.3(1); N1−Ni1−Cl1A, 96.1(2); P1−Ni1−Cl1A, 177.4(1); Cl1−Ni1−Cl1A, 85.5(1); Ni1−Cl1−Ni1A, 94.5(1).

coordination geometry about nickel in **2d** is best described as distorted square planar, in which the Cl1A is datively bound to Ni1, as evidenced by its relatively longer bond length of 0.071 Å in comparison to that of Ni1−Cl1. The two datively bound donors at nickel are thus mutually trans to each other, so are the two formally anionic donors. The two *o*-phenylene rings lie approximately on the same plane as the Ni_2Cl_2 rectangle, wherein the two nickel atoms are separated by 3.277 Å. The N-bound aryl and P-bound isopropyl groups are oriented virtually axially or nearly perpendicular to the *o*-phenylene rings, thereby creating significant steric protection for the nickel center at axial positions. Other structural parameters are unexceptional. A similar structure was also reported previously for a bromide-bridged molecule.[38]

In contrast to **2b−d**, complex **2a** remains elusive. Surprisingly, reactions employing H[**1a**][36] or Li[**1a**](THF)$_2$[33] with strategies illustrated in eq 1 led instead to high-yield isolation of dark red prismatic Ni[**1a**]$_2$ (**3a**), as indicated by X-ray diffraction analysis. Compound **3a** is ^{31}P NMR silent, reflective of its paramagnetic nature. In principle, the presumed nickel chloride **2a** was also produced from the reactions attempted. We reason that **2a**, however, is transient and inherently much more reactive than **2b−d** to react with a second equivalent of their corresponding protio or lithium precursors, even if the reactions were conducted with equimolar starting materials. Close scrutiny of the reaction progress by ^{31}P{^{1}H} NMR spectroscopy revealed no observable intermediates by the lithium route[39] but occurrence of an intermediate in the other strategy in <30 min, as evidenced by a signal found at 32.0 ppm, presumably **2a**. Attempts to selectively isolate the presumed **2a** were not successful. Both electronic and steric factors were considered to rationalize the higher reactivity of **2a** in comparison to that of **2b−d**. On electronic grounds, the nickel center in the former is more electron deficient due to the incorporation of electronically less releasing substituents at the NP donor atoms. Sterically, these substituents are not bulky enough to prevent **2a** from further reactions that give ultimately the homoleptic **3a**. This result is consistent with what was demonstrated previously on the overall steric size of these NP ligands following the order **1a** < **1b** < **1c** < **1d**.[35]

Figure 3 depicts the molecular structure of this homoleptic complex. The coordination geometry of **3a** is severely distorted

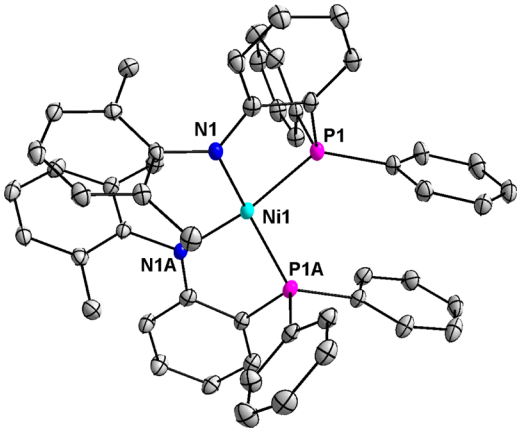

Figure 3. Molecular structure of **3a** with thermal ellipsoids drawn at the 35% probability level. Selected bond distances (Å) and angles (deg): Ni1−N1, 1.965(2); Ni1−P1, 2.1588(8); N1−Ni1−N1A, 105.6(1); N1−Ni1−P1A, 153.00(7); N1−Ni1−P1, 83.34(7); P1A−Ni1−P1, 100.32(4).

from both square planar and tetrahedral, having a dihedral angle between two N1−Ni1−P1 planes of 40.89°: i.e., a structure approximately halfway between these idealized extremes. The same conclusion is also derived from Houser's four-coordinate geometry index τ_4[40] of 0.38 for this molecule. Such a distortion from the ideal square planar or tetrahedral structures likely has something to do with the $\pi-\pi$ stacking (Figure S1; see the Supporting Information) that involves two amido aryls (ring centroid distance 3.484 Å) or P-bound phenyl groups (ring centroid distance 3.464 Å). Though bis-ligated nickel complexes of [**1b−d**]$^-$ were not produced under the conditions examined, these ligands, on the other hand, do show a much higher propensity to give exclusively homoleptic derivatives of zinc[35] upon reactions of their corresponding lithium complexes with ZnX_2 (X = Cl, OAc), regardless of the stoichiometry of the starting materials employed. In particular, Zn[**1d**]$_2$ rather than {[**1d**]Zn(μ-Cl)}$_2$ or {[**1d**]Zn(μ-OAc)}$_2$ was isolated, though this homoleptic complex is severely congested sterically, as demonstrated by X-ray diffraction analysis.[35] The remaining structural parameters of **3a** are unexceptional.

Direct alkylation of **2b−d** with nonchelating[41] Grignard reagents (1 equiv per nickel) was attempted. Though reactions involving those lacking β-hydrogen atoms appear to proceed smoothly (e.g., treating **2c** with MeMgCl in THF at −35 °C led to quantitative formation of a new species whose ^{31}P{^{1}H} NMR spectrum shows a singlet at 55 ppm), identification of the products produced is thus far inconclusive. Similar reactions employing β-hydrogen-containing Grignard reagents, on the

dx.doi.org/10.1021/om5006353 | *Organometallics* XXXX, XXX, XXX−XXX

Scheme 1. Synthesis of PMe_3 Adducts of Nickel Chlorides 4b,c and Methyls 5b,c

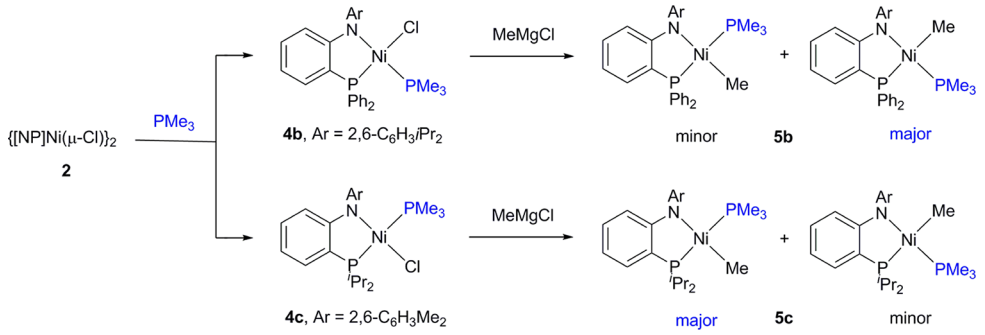

other hand, gave mixtures of products as indicated by $^{31}P\{^1H\}$ NMR studies. Characterization or purification of these mixtures proved problematic.

The most effective strategy in these pursuits involves the participation of an exogenous Lewis base. Upon addition of PMe_3 in THF at room temperature, the red solutions of **2b,c** turned green, from which emerald crystals of [**1b,c**]NiCl(PMe_3) (**4b,c**) were isolated in high yields (Scheme 1). Subsequent alkylation of **4b,c** with RMgCl (R = Me, CH_2SiMe_3, Ph) in THF at −35 °C successfully afforded high yields of [**1b,c**]NiR(PMe_3) (R = Me (**5b,c**), CH_2SiMe_3 (**6b,c**), Ph (**7b,c**)) as red or brownish red crystals. Interestingly, treating **4c** with EtMgCl or *n*BuMgCl under similar conditions yielded instead the hydrido species [**1c**]NiH(PMe_3) (**8c**) quantitatively; analysis of the reaction progress with time by $^{31}P\{^1H\}$ NMR spectrometry in THF revealed in each of these reactions the formation of an intermediate that we tentatively formulated as [**1c**]NiEt(PMe_3)[42] and [**1c**]Ni*n*Bu(PMe_3),[43] respectively, in view of the resemblance of their chemical shifts and phosphorus−phosphorus coupling constants to what was observed for alkylated major-**5c** and **6c** (Table 1). Attempts to isolate the presumed [**1c**]NiEt(PMe_3) or [**1c**]Ni*n*Bu(PMe_3) were not successful due to the inevitably concomitant presence of either **4c** or **8c**. The generation of hydrido compound **8c** is apparently a consequence of *β*-hydrogen elimination of these organonickel species. Note that this *β*-elimination is facile, as **8c** begins to evolve in <15 min, as indicated by $^{31}P\{^1H\}$ NMR studies. This result is in sharp contrast to what was found in the PNP and PNN systems, wherein *β*-hydrogen-containing organonickel complexes are thermally stable[29−32] even at elevated temperatures (e.g., 70 °C). The reactivity of hydrido species **8c** with respect to olefin insertion was also examined. In the presence of 1-hexene (3 equiv, 25−60 °C in C_6D_6), **8c** appears to remain intact, as indicated by $^{31}P\{^1H\}$ NMR studies. Examination of these reaction mixtures by ^1H NMR and GC/MS analyses, however, confirmed the production of oligo(1-hexene), thereby revealing the catalytic nature of **8c** in 1-hexene oligomerization that involves 1-hexene polyinsertion followed by *β*-hydrogen elimination. Note that the presumed [**1c**]Ni(hexyl)(PMe_3) was not observed spectroscopically. Collectively, *β*-elimination of [**1c**]Ni(CH_2CH_2R)(PMe_3) to produce **8c** is thus thermodynamically downhill. In comparison with those compounds derived from PNP and PNN, this present result is attributable to the lack of a third donor atom in the amido phosphine chelates incorporated. Though overall four-coordinate in conformation, the nickel center in **8c** and its presumed olefin insertion products possesses, upon PMe_3 dissociation,[44,45] a vacant d orbital that is low-lying in energy available to either olefin coordination or *β*-hydrogen elimination, respectively. The hydrido species **8c** could alternatively be prepared from the reaction of **4c** with $LiHBEt_3$.

Though a wide variety of exogenous Lewis bases are synthetically useful to facilitate the preparation of organonickel complexes in this study, the inclusion of a phosphine, e.g., PMe_3 in the current case, in these four-coordinate species provides an excellent probe to investigate their thermodynamic preference in stereochemistry by the $^2J_{PP}$ values acquired from $^{31}P\{^1H\}$ NMR spectra of reaction aliquots. In principle, two possible geometric isomers may be produced, i.e., cis and trans, as defined by the orientation of the two phosphorus donors incorporated. Interestingly, $^{31}P\{^1H\}$ NMR studies of all complexes described herein revealed the presence of only one of these possible isomers in solution, except for the methyl complexes **5b,c**. Though both isomers were observed for **5b,c**, the cis:trans ratio of the former is ca. 9:1 whereas that of the latter is <1:11, as estimated by the relative intensities of two pairs of doublet resonances observed in their corresponding $^{31}P\{^1H\}$ NMR spectra. As summarized in Table 1, the major isomer of **5b** exhibits in the $^{31}P\{^1H\}$ NMR spectrum two doublet resonances with a coupling constant of 25 Hz, while that of **5c** shows a $^2J_{PP}$ value of 296 Hz. For those existing as a single isomer, the chloro **4b** is the only cis-disposed complex, whereas the others are all trans. In other words, all $[\mathbf{1c}]^-$-derived PMe_3 adducts of nickel reported herein are trans-disposed except for the minor isomer of the methyl species **5c**. With the coordination of $[\mathbf{1b}]^-$, the trimethylsilyl compound **6b**, phenyl compound **7b**, and the minor isomer of methyl **5b** are trans but the chloro species **4b** and the major isomer of **5b** are cis. As a result, the isomeric preference of these nickel complexes is clearly a function of the identity of both NP and the monodentate anionic ligands (i.e., Cl, alkyl, Ph, H) incorporated.

The ^1H and $^{13}C\{^1H\}$ NMR data are also informative in determining the solution structures of these PMe_3 adducts. In general, these complexes are characteristic of having a time-averaged C_s-symmetric structure; for instance, only one set of signals is observed for the two *o*-alkyl groups in the amido substituents. The hydrido ligand in **8c** and the H_α/C_α atoms in complexes **5**−**7** generally give rise to a diagnostic doublet of doublets resonance; for instance, the former ligand resonates characteristically at −20 ppm with $^2J_{HP}$ values of 73 and 82 Hz. These data are all quite comparable to those of [PNP]NiH, particularly the species that carries different substituents at the two phosphorus donors,[30] thus emphasizing the cis-disposed orientation of the hydride ligand in **8c** with respect to these phosphorus atoms. Collectively, these NMR data are all consistent with a solution structure having square-planar geometry.

X-ray studies of complexes **4**−**8** were attempted to elucidate the solid-state structures of these molecules and to evaluate the

dx.doi.org/10.1021/om5006353 | *Organometallics* XXXX, XXX, XXX−XXX

possibilities of resolving the decisive factors that determine their preferred stereochemistry. Methods to grow X-ray-quality crystals of these complexes are addressed in the Experimental Section. The molecular structures of **4c**, **5c**, **6b,c**, **7c**, and **8c** are depicted in Figures 4−9, while those of **4b**, **5b**, and **7b** were

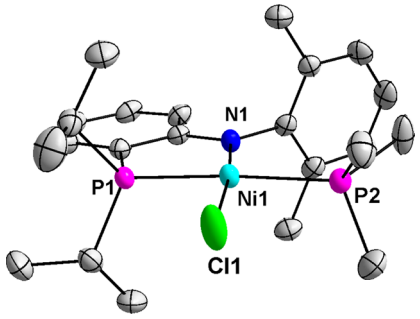

Figure 4. Molecular structure of **4c** with thermal ellipsoids drawn at the 35% probability level.

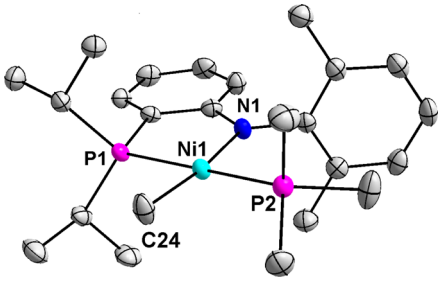

Figure 5. Molecular structure of **5c** with thermal ellipsoids drawn at the 35% probability level.

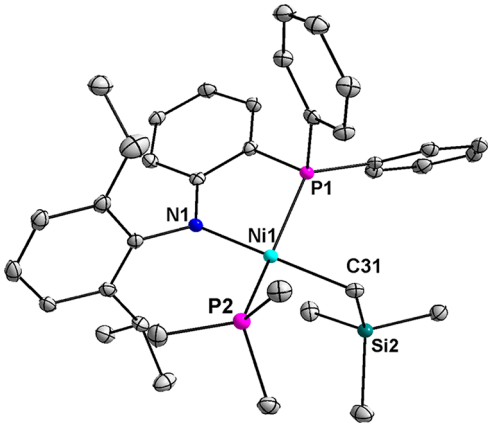

Figure 6. Molecular structure of **6b** with thermal ellipsoids drawn at the 35% probability level.

reported previously.[33] For a comprehensive comparison, selected bond distances and angles are summarized in Tables 2 and 3, respectively. Consistent with what was deduced from the solution NMR studies, the coordination geometry of these PMe_3 adducts is best described as distorted square planar, wherein the two phosphorus donors in **4c**, **5c**, **6b,c**, **7b,c**, and **8c** are mutually trans while those in **4b** and **5b** are cis. The resolved X-ray structures of methyl species **5b** and **5c** agree well with their corresponding major isomers observed in solution. In general, the nickel center in chloro compounds **4b,c** and methyl compounds **5b,c** lies perfectly on the mean coordination plane

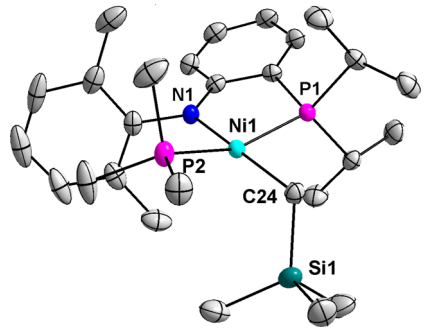

Figure 7. Molecular structure of **6c** with thermal ellipsoids drawn at the 35% probability level.

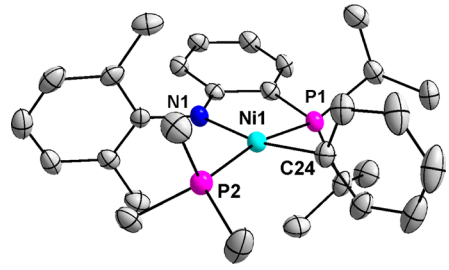

Figure 8. Molecular structure of **7c** with thermal ellipsoids drawn at the 35% probability level.

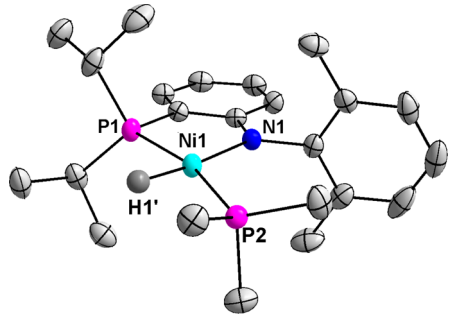

Figure 9. Molecular structure of **8c** with thermal ellipsoids drawn at the 35% probability level.

defined by four donor atoms, whereas that in trimethylsilylmethyl species **6b,c** and phenyl species **7b,c** is displaced by 0.142, 0.179, 0.052, and 0.017 Å, respectively. This phenomenon is ascribable to the distinct steric sizes of Cl, Me, CH_2SiMe_3, and Ph incorporated in these molecules. In particular, the core geometry of the trimethylsilylmethyl species **6b,c** is severely distorted from the ideal square planar, with P1−Ni−P2 angles of 151.36(4) and 155.22(3)°, respectively.

Though severely distorted, the X-ray structures of **6b,c** signify clearly their preferred stereoisomer in the ground state. It has been demonstrated that the steric size of substituents in these *o*-phenylene-derived ligands follows the order $PiPr_2$ > $N(C_6H_3iPr_2\text{-}2,6)$ > $N(C_6H_3Me_2\text{-}2,6)/PPh_2$.[35] Assuming a structure with lessened steric congestion is preferred, complex **6c** would have adopted an orientation wherein the sterically demanding trimethylsilylmethyl group and the comparatively large $PiPr_2$ moiety are trans, leaving in turn the two phosphorus donors being cis. The fact that the phosphorus donors in **6c** are trans-disposed is thus ascribable to electronic reasons: the two formally anionic donors prefer a trans orientation, as do the two datively bound phosphorus atoms. This preferred stereochemical orientation appears to be general in this series of compounds, as

dx.doi.org/10.1021/om5006353 | *Organometallics* XXXX, XXX, XXX−XXX

Table 2. Selected Bond Distances (Å) for [1]NiX(PMe_3) (4−8)

compd	X	Ni−N	Ni−P1	Ni−P2	Ni−X[a]
4b[b]	Cl	1.923(3)	2.156(1)	2.194(1)	2.201(1)
5b[b]	Me	1.939(3)	2.201(1)	2.148(1)	2.035(4)
6b	CH_2SiMe_3	1.956(3)	2.1578(9)	2.2162(9)	1.980(3)
7b[b]	Ph	1.947(5)	2.149(2)	2.238(2)	1.923(7)
4c	Cl	1.893(2)	2.1744(8)	2.2979(8)	2.1957(9)
5c	Me	1.956(3)	2.153(1)	2.242(1)	1.980(4)
6c	CH_2SiMe_3	1.972(2)	2.1556(8)	2.2549(8)	1.979(3)
7c	Ph	1.948(5)	2.171(2)	2.242(2)	1.916(7)
8c	H	1.915(2)	2.1304(9)	2.1712(9)	1.4489

[a]Data reported involve the donor atom of the X ligand specified. [b]Data selected from ref 33.

Table 3. Selected Bond Angles (deg) for [1]NiX(PMe_3) (4−8)

compd	X	N−Ni−P1	N−Ni−X[a]	N−Ni−P2	P1−Ni−X[a]	P1−Ni−P2	P2−Ni−X[a]
4b[b]	Cl	85.21(9)	93.54(9)	175.2(1)	177.68(5)	97.51(4)	83.85(5)
5b[b]	Me	85.0(1)	92.2(2)	173.5(1)	176.4(1)	99.36(5)	83.7(1)
6b	CH_2SiMe_3	83.81(8)	162.3(1)	104.97(8)	90.0(1)	151.36(4)	88.3(1)
7b[b]	Ph	85.5(2)	167.6(3)	105.1(2)	85.7(2)	163.76(9)	85.1(2)
4c	Cl	85.46(8)	172.07(8)	102.86(8)	87.32(3)	171.68(3)	84.37(3)
5c	Me	85.10(9)	171.8(1)	102.64(9)	87.0(1)	170.69(4)	85.1(1)
6c	CH_2SiMe_3	85.19(7)	169.5(1)	98.22(7)	88.43(9)	155.22(3)	91.13(9)
7c	Ph	85.4(2)	168.8(3)	102.3(2)	87.7(2)	168.58(8)	85.9(2)
8c	H	86.70(8)	172.3	108.69(8)	85.8	164.20(4)	78.9

[a]Data reported involve the donor atom of the X ligand specified. [b]Data selected from ref 33.

exemplified by dimeric chloro species **2d** and all PMe_3 adducts, except **4b** and major-**5b**. Consistent with this rationale, Alcock also argued that primary bonds (e.g., Ni−N and Ni−X in this study, X = Cl (**4**), Me (**5**), CH_2SiMe_3 (**6**), Ph (**7**), H (**8**)) are more stereochemically active than secondary bonds[46] (e.g., Ni−P in this study) in dictating the primary coordination geometry.

Though electronic factors predominate in dictating the cis/trans geometry of these four-coordinate species, the steric nature of ligands incorporated therein deserves more comment. While electronic and steric factors play contrary roles for **6c** in this regard, these considerations lead instead to the same preference in **6b**, as both formally anionic donors, i.e., CH_2SiMe_3 and N($C_6H_3iPr_2$-2,6), are characteristic of the largest and the second largest in this molecule. In contrast, the sterically much smaller Cl and Me ligands in **4b** and major-**5b**, respectively, take on a position that is sterically favored; i.e., the two relatively large N($C_6H_3iPr_2$-2,6) and PMe_3 donors are trans, rendering two datively bound phosphorus donors cis-disposed. Such a preference in cis-disposed phosphine ligands appears exceptional. In a separate study, Klein et al. also demonstrated that trans isomers of chloro species **4e,f** and methyl compound **5e−h** (eq 2) are dominant in solution.[44] A similar preference for

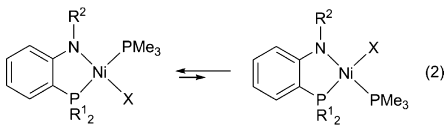

the trans configuration was also reported for their *o*-phosphinophenolate congeners.[45] The reason why sterics dominates in **4b** and major-**5b** is not clear at this stage. It is likely that, however, the energy differences in these cis/trans isomers could be fairly small, allowing the cis/trans equilibria to be established readily in solution.

The reactivity of chloro species **2b−d** with respect to Kumada couplings was examined. Table 4 summarizes the survey of reaction parameters with an *n*-butyl nucleophile and a phenyl electrophile as prescribed building blocks. We chose to assess the compatibility of this model reaction with both polar and nonpolar solvents under ambient and elevated temperature conditions. In general, these chloro complexes are all competent catalyst precursors for Kumada couplings, yielding *n*-butylbenzene as the desirable product. Regardless of the identity of NP, reactions conducted in THF and DME at 60 °C are consistently superior to the others investigated (Table 4) in view of higher reactivity and selectivity. On the other hand, complex **2d** (entry 24) outperforms **2b** (entry 4) and **2c** (entry 14), producing *n*-butylbenzene nearly quantitatively and selectively. The high-yield production of *n*-butylbenzene in this catalysis is particularly remarkable, given the fact that *β*-elimination is a facile thermodynamic process, as indicated by the stoichiometric chemistry established (vide supra).

Led by the results concluded in Table 4, we attempted to probe the reaction scope employing catalytic **2d** in THF at 60 °C. As presented in Table 5, both alkyl and aryl Grignard reagents are compatible nucleophiles to couple with phenyl chloride, bromide, and iodide efficiently and selectively. In particular, chlorobenzene, which is characteristic of a synthetically more challenging electrophile, could be successfully coupled with 4-tolyl, 2-tolyl, and *n*-butyl Grignard reagents (entries 3, 6, and 9, respectively). Interestingly, this inherently inert electrophile gives reactivity and selectivity comparable to that of bromo- and iodobenzene upon reaction with 4-tolyl nucleophile (entries 1−3). Steric repulsion imposed by ortho substituents in tolyl Grignard reagents does not appear to affect catalysis much (entries 1 and 2 versus entries 4 and 5) except those involving chlorobenzene (entry 3 versus entry 6) in terms of conversion rates. Nevertheless, the selectivities to produce cross-coupled products were found to be virtually identical in these reactions (entries 1−6).

dx.doi.org/10.1021/om5006353 | *Organometallics* XXXX, XXX, XXX−XXX

Table 4. Survey of Reaction Parameters for Kumada Couplings by Catalytic 2b–d[a]

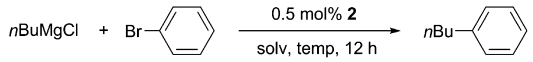

entry	2	solvent	temp (°C)	conversn (%)[b]	*n*BuPh/biphenyl selectivity[b]
1	**2b**	Et_2O	25	2	71/29
2	**2b**	Et_2O	reflux	83	42/58
3	**2b**	THF	25	24	84/16
4	**2b**	THF	60	98	82/18
5	**2b**	DME	25	70	73/27
6	**2b**	DME	60	98	85/15
7	**2b**	1,4-dioxane	25	15	95/5
8	**2b**	1,4-dioxane	60	82	83/17
9	**2b**	toluene	25	0	0/0
10	**2b**	toluene	60	10	83/17
11	**2c**	Et_2O	25	2	60/40
12	**2c**	Et_2O	reflux	35	52/48
13	**2c**	THF	25	59	71/29
14	**2c**	THF	60	100	85/15
15	**2c**	DME	25	62	72/28
16	**2c**	DME	60	100	77/23
17	**2c**	1,4-dioxane	25	16	93/7
18	**2c**	1,4-dioxane	60	30	92/8
19	**2c**	toluene	25	1	56/44
20	**2c**	toluene	60	8	83/17
21	**2d**	Et_2O	25	11	98/2
22	**2d**	Et_2O	reflux	26	91/9
23	**2d**	THF	25	16	91/9
24	**2d**	THF	60	100	98/2
25	**2d**	DME	25	28	80/20
26	**2d**	DME	60	94	88/12
27	**2d**	1,4-dioxane	25	24	89/11
28	**2d**	1,4-dioxane	60	82	76/24
29	**2d**	toluene	25	0	0/0
30	**2d**	toluene	60	5	83/17

[a]All reactions were carried out with 0.11 M phenyl bromide and 0.12 M *n*-butylmagnesium chloride in 2 mL of solvent at the prescribed temperature. [b]Determined by GC, based on phenyl bromide; average of two runs.

Table 5. Kumada Couplings by Catalytic 2d[a]

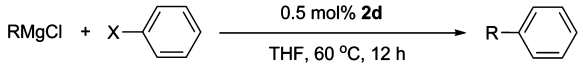

entry	R	X	conversn (%)[b]	R-Ph/Ph-Ph selectivity[b]
1	4-tolyl[c]	I	94	95/5
2	4-tolyl[c]	Br	89	93/7
3	4-tolyl[c]	Cl	89	93/7
4	2-tolyl	I	92	99/1
5	2-tolyl	Br	93	99/1
6	2-tolyl	Cl	65	95/5
7	*n*-Bu	I	100	82/18
8	*n*-Bu	Br	100	98/2
9	*n*-Bu	Cl	75	100/0
10	Et	I	100	70/30

[a]Unless otherwise noted, all reactions were carried out with 0.11 M phenyl halide and 0.12 M Grignard reagent in 2 mL of THF. [b]Determined by GC, based on phenyl halides; average of two runs. [c]4-Tolylmagnesium bromide was used.

The success in satisfactorily yielding cross-coupled products with β-hydrogen-containing building blocks (entries 7–10 in Table 5) is remarkable, as β-elimination in this system is thermodynamically favorable due to the lack of a third donor such as what PNP and PNN possess. These intriguing results, however, strongly argue that the kinetic rate of catalytic Kumada couplings is much higher than that of β-elimination in this NP system. The kinetic rates of olefin insertion involving nickel hydrides should be even slower, and thus the possibilities of cross-couplings involving β-elimination followed by olefin reinsertion[47] can be ruled out. The high-yield production of these alkylated arenes also strongly implies that monoalkyl nickel complexes of the type [**1**]$NiCH_2CH_2R(L)$ (L = solvent or other datively bound donors available in reaction solutions) are not key intermediates responsible for this cross-coupling catalysis, particularly taking into account that the couplings were conducted at elevated temperatures (60 °C in this case) that in principle should facilitate β-elimination. To gain more insights, controlled experiments employing catalytic PMe_3-bound **4c** (1 mol %) were conducted under conditions otherwise identical with those for reactions catalyzed by dimeric **2c** (Table 4, entry 14). Interestingly, though **4c** and **2c** gave virtually identical selectivities in *n*-butylbenzene production (87% versus 85%), the former apparently reacts much more slowly than the latter (23% versus 100% conversion), likely reflecting the necessity of dissociation or nucleophilic substitution of the coordinated PMe_3 in the former. Nevertheless, the nearly identical selectivities of **4c** and **2c** imply possibly the same operative mechanism. It is also interesting to compare the catalytic activity of **4c** with those of [PNP]NiCl[29] in Kumada couplings, given the fact that both catalysts are composed of two trans-disposed phosphorus donors. In this regard, **4c** was found to have much lower turnover rates but significantly higher selectivities in *n*-butylbenzene formation, clearly indicating that the Kumada couplings by NP- and PNP-derived nickel catalysts are mechanistically distinctive.

We reason instead that the double-alkylated ate complexes $\{$[**1**]$Ni(CH_2CH_2R)_2\}^-$ play an important role in this Kumada coupling in view of the potentially facile alkylation rates of [**1**]$NiCH_2CH_2R(L)$ and the lack of an empty, low-lying d orbital in $\{$[**1**]$Ni(CH_2CH_2R)_2\}^-$ that discourages β-elimination. In line with this, reactions of dimeric **2c** with 4 equiv of either *n*BuMgCl or Me_3SiCH_2MgCl in THF at 25 °C were attempted. Unfortunately, these reactions gave a mixture of products as evidenced by ^1H and $^{31}P\{^1H\}$ NMR studies, from which the product conformations could not be deduced conclusively. The $^{31}P\{^1H\}$ NMR spectra of these reaction aliquots, however, clearly indicated that these products are conformationally distinctive from those derived from analogous reactions employing 2 equiv of corresponding Grignard reagents, consistent with the proposal that the monoalkyl species [**1c**]NiR(L) reacts with another 1 equiv of RMgX to give a nickelate complex. The participation of anionic nickelate species in cross-coupling catalysis has also been proposed and discussed in several studies.[48−51] With the accumulated negative charge, the ate complexes $\{$[**1**]$Ni(CH_2CH_2R)_2\}^-$ are in principle much better nucleophiles than [**1**]$NiCH_2CH_2R(L)$ to react with halo electrophiles, thus bypassing the thermodynamically favorable β-elimination of [**1**]$NiCH_2CH_2R$-(L) found in stoichiometric reactions.

Alternatively, the presumed $\{$[**1**]$Ni(CH_2CH_2R)_2\}^-$ may undergo reductive elimination to give $\{$[**1**]$Ni\}^-$ that contains a formally zerovalent nickel, which in turn reacts with PhX to generate [**1**]NiPh and X^- via oxidative addition. Subsequent nucleophilic attack of RMgX to [**1**]NiPh then possibly affords

dx.doi.org/10.1021/om5006353 | *Organometallics* XXXX, XXX, XXX–XXX

the ate complex intermediates $\{[\mathbf{1}]Ni(Ph)(R)\}^-$ ready for R-Ph production and $\{[\mathbf{1}]Ni\}^-$ regeneration. To briefly assess the validity of this hypothesis, controlled experiments employing **7c** with 1 equiv of *n*BuMgCl or 4-tolylMgBr in THF at 60 °C were conducted. Indeed, these reactions produced in 12 h *n*-butylbenzene in nearly quantitative yield and 4-methylbiphenyl in 95% selectivity, respectively, as evidenced by GC/MS analyses on organic products of reaction aliquots. Interestingly, these selectivity results are quite comparable to those obtained under similar but catalytic conditions (Table 5, entries 8 and 9 and entries 1−3, respectively).

The somewhat superior reactivity and selectivity of **2d** in comparison to those of **2b,c** (entries 4, 14, and 24 in Table 4) thus likely reflect the electronic discrepancy of the presumed nickelate complexes $\{[\mathbf{1b-d}]Ni(CH_2CH_2R)_2\}^-$ or $\{[\mathbf{1b-d}]Ni\}^-$. Perhaps more importantly, the nucleophilicity of $\{[\mathbf{1d}]Ni(CH_2CH_2R)_2\}^-$ or $\{[\mathbf{1d}]Ni\}^-$ is sufficiently capable of activating the intrinsically challenging $C(sp^2)-Cl$ bond (entries 3, 6, and 9 in Table 5), giving selectively the desirable cross-coupled products. Notably, these results are in sharp contrast to what was observed for both PNP and PNN, wherein Kumada catalysis employing chloro electrophiles proceeds barely or unsatisfactorily.[29,32] Mechanistically, the participation of radicals in this catalysis was considered. In the presence of typical radical inhibitors such as 2,6-di-*tert*-butyl-4-hydroxytoluene or 2,2,6,6-tetramethyl-1-piperidinyloxy (1 equiv to halo electrophiles), the catalytic activity and selectivity remain virtually identical (e.g., entry 10 in Table 5), thereby precluding radical involvement in this process.

CONCLUSIONS

We have prepared and structurally characterized a series of divalent nickel complexes containing bidentate diarylamido phosphine ligands. Of the complexes characterized in this study, **3a** is the only homoleptic species that is paramagnetic in nature. As elucidated by X-ray crystallography, the coordination geometry of **3a** is approximately halfway between ideal tetrahedral and square planar. With $[\mathbf{1b-d}]^-$ ligands that are sterically larger and electronically more releasing than $[\mathbf{1a}]^-$, all other nickel derivatives are diamagnetic mono-NP complexes whose core structure is best described as square planar, as confirmed by solution NMR and single-crystal X-ray studies. Incorporation of an exogenous PMe_3 in these square-planar species facilitates the synthesis of organonickel complexes and the identification of their possible cis/trans stereoisomers in solution. Electronic factors were found to play a major role in dictating cis/trans preferences of these square-planar species: the two formally anionic donors prefer a trans orientation, as do the two datively bound atoms. In contrast to what was found for PNP and PNN systems,[29−32] β-hydrogen elimination is thermodynamically favorable in this study. As a result, organonickel derivatives were all found not to contain β-hydrogen atoms, as exemplified by complexes **5**−**8**. Nevertheless, the chloro complexes **2** are all competent catalyst precursors for Kumada couplings, including those employing β-hydrogen-containing building blocks. Remarkably, the synthetically more challenging chlorobenzene is also a compatible electrophile in this catalysis. The NP complexes are thus superior catalysts to their PNP or PNN congeners[29,32] in this regard. We propose that the formation of anionic nickelate complexes $\{[\mathbf{1}]Ni(CH_2CH_2R)_2\}^-$ and $\{[\mathbf{1}]Ni\}^-$ is crucial to facilitate such intriguing reactivity; i.e., catalytic Kumada couplings are kinetically preferred to thermodynamically favorable β-hydrogen elimination.

EXPERIMENTAL SECTION

General Procedures. Unless otherwise specified, all experiments were performed under nitrogen using standard Schlenk or glovebox techniques. All solvents were reagent grade or better and were purified by standard methods. The compounds $NiCl_2(DME)$,[34] H[**1a**],[36] H[**1b**],[37] H[**1c**],[35] H[**1d**],[35] [**1a**]Li(THF)$_2$,[33] [**1b**]Li(THF)$_2$,[37] [**1c**]Li(THF)$_2$,[35] [**1d**]Li(DME),[35] **2b**,[33] **4b**,[33] **5b**,[33] and **7b**[33] were prepared according to literature procedures. All other chemicals were obtained from commercial vendors and used as received. All NMR spectra were recorded at room temperature in specified solvents on Varian Unity or Bruker AV instruments. Chemical shifts (δ) are listed as parts per million downfield from tetramethylsilane, and coupling constants (J) and peak widths at half-height ($\Delta\nu_{1/2}$) are in hertz. Routine coupling constants are not listed. ^{1}H NMR spectra are referenced using the residual solvent peak at δ 7.16 for C_6D_6. ^{13}C NMR spectra are referenced using the internal solvent peak at δ 128.39 for C_6D_6. The assignment of the carbon atoms for all compounds is based on DEPT ^{13}C NMR spectroscopy. ^{31}P NMR spectra are referenced externally using 85% H_3PO_4 at δ 0. The Kumada coupling reactions were analyzed by GC on a Varian Chrompack CP-3800 instrument equipped with a CP-Sil 5 CB chrompack capillary column or by GC/MS on a Varian 450-GC/240-MS instrument equipped with a Restek MXT-5 column. The identity of the cross-coupling products was confirmed by comparison with authentic samples. GC yields were quantified by signal integrals relative to those of prescribed amounts of eicosane as an internal standard. Elemental analysis was performed on a Heraeus CHN-O Rapid analyzer.

X-ray Crystallography. Crystallographic data for **2d**, **3a**, **4c**, **5c**, **6b,c**, **7c**, and **8c** (CCDC reference numbers 999526−999533) are summarized in the Supporting Information. Data were collected on a diffractometer with graphite-monochromated Mo Kα radiation (λ = 0.7107 Å). Absorption correction was applied using SADABS.[52] Structures were solved by direct methods and refined by full-matrix least-squares procedures against F^2 using SHELXL-97.[53] All full-weight non-hydrogen atoms were refined anisotropically. Hydrogen atoms were placed in calculated positions. The structure of **2d** contains disordered CH_2Cl_2. Attempts to obtain suitable disorder models failed. The SQUEEZE procedure of the Platon program was used to obtain a new set of F^2 (hkl) values without the contribution of solvent molecules.[54]

Synthesis of {[1c]Ni(μ-Cl)}$_2$ (2c). *Method 1.* A THF solution (5 mL) of H[**1c**] (500 mg, 1.60 mmol) and neat NEt_3 (243 mg, 2.40 mmol, 1.5 equiv) was sequentially added to a suspension of $NiCl_2(DME)$ (352 mg, 1.60 mmol) at room temperature. After being stirred at room temperature for 1 h, the reaction mixture was evaporated to dryness under reduced pressure. The residue was triturated with pentane (3 mL × 2), and benzene (16 mL) was added. The benzene solution was filtered through a pad of Celite and evaporated to dryness in vacuo. The solid thus obtained was washed with pentane and dried in vacuo to give the desired product as a brick red solid; yield 605 mg (93%).

Method 2. Solid $NiCl_2(DME)$ (48.3 mg, 0.22 mmol) was suspended in THF (3 mL) and cooled to −35 °C. To this was added dropwise a solution of [**1c**]Li(THF)$_2$ (100 mg, 0.22 mmol) in THF (3 mL) at −35 °C. Upon addition, the reaction mixture turned red and the suspended $NiCl_2(DME)$ dissolved. The solution was stirred at room temperature overnight. All volatiles were removed in vacuo. The resulting residue was dissolved in benzene (6 mL). The benzene solution was passed through a pad of Celite and evaporated to dryness in vacuo to afford the product as a brick red solid; yield 51.2 mg (58%). ^{1}H NMR (C_6D_6, 500 MHz): δ 7.04 (br s, 6, Ar), 6.71 (m, 4, Ar), 6.23 (t, 2, Ar), 5.70 (m, 2, Ar), 2.60 (s, 12, ArCH_3), 1.61 (m, 4, CHMe$_2$), 1.36 (m, 12, CHMe_2), 1.22 (m, 12, CHMe_2). ^{31}P{^{1}H} NMR (C_6D_6, 202.3 MHz): δ 62.6 ($\Delta\nu_{1/2}$ = 27). ^{13}C{^{1}H} NMR (C_6D_6, 125.5 MHz): δ 167.3 (d, J_{CP} = 17.8, C), 149.0 (s, C), 138.0 (s, C), 134.2 (s, CH), 131.3 (s, CH), 129.0 (s, CH), 124.8 (s, CH), 113.5 (d, J_{CP} = 4.0, CH), 112.5 (s, CH), 110.0 (d, J_{CP} = 49.8, C), 25.9 (d, $^1J_{CP}$ = 24.4, CHMe$_2$), 19.8 (s, CHMe_2), 18.6 (s, CHMe_2), 17.8 (s, ArCH_3).

dx.doi.org/10.1021/om5006353 | Organometallics XXXX, XXX, XXX−XXX

Anal. Calcd for $(C_{40}H_{54}Cl_2N_2Ni_2P_2)(C_6H_6)(C_4H_8O)_2$: C, 62.62; H, 7.40; N, 2.71. Found: C, 62.85; H, 7.42; N, 2.95.

Synthesis of {[1d]Ni(μ-Cl)}$_2$ (2d). The experimental procedures were similar to those of **2c**, employing H[**1d**] (in CH_2Cl_2 instead of THF) and [**1d**]Li(DME) in place of H[**1c**] and [**1c**]Li(THF)$_2$, respectively: yield of method 1 74%, yield of method 2 79%. ^{1}H NMR (C_6D_6, 500 MHz): δ 7.17 (m, 6, Ar), 6.67 (t, 2, Ar), 6.63 (t, 2, Ar), 6.06 (t, 2, Ar), 5.65 (d, 2, Ar), 4.04 (septet, 4, C*H*Me$_2$), 1.88 (d, 12, CH*Me*$_2$), 1.64 (br m, 4, C*H*Me$_2$), 1.43 (m, 12, CH*Me*$_2$), 1.19 (d, 24, CH*Me*$_2$). ^{31}P{^{1}H} NMR (C_6D_6, 202.3 MHz): δ 60.2. ^{13}C{^{1}H} NMR (C_6D_6, 125.5 MHz): δ 168.7 (d, J_{CP} = 21.0, C), 147.9 (s, C), 145.6 (s, C), 133.5 (s, CH), 131.2 (s, CH), 125.9 (s, CH), 124.1 (s, CH), 115.4 (d, J_{CP} = 8.7, CH), 112.5 (s, CH), 109.4 (d, J_{CP} = 51.2, C), 29.1 (s, CH), 25.7 (d, J_{CP} = 26.1, CH), 24.9 (s, CH_3), 24.9 (s, CH_3), 18.4 (s, CH_3), 17.5 (s, CH_3). Anal. Calcd for $C_{48}H_{70}Cl_2N_2Ni_2P_2$: C, 62.28; H, 7.63; N, 3.03. Found: C, 62.24; H, 7.70; N, 3.08.

Synthesis of Ni[1a]$_2$ (3a). The experimental procedures were similar to those of **2c**, employing H[**1a**] and [**1a**]Li(THF)$_2$ in place of H[**1c**] and [**1c**]Li(THF)$_2$, respectively: yield of method 1 60%, yield of method 2 78%. After multiple attempts even with X-ray-quality crystals, we were not able to obtain satisfactory analysis data for this compound. Anal. Calcd for $C_{52}H_{46}N_2NiP_2$: C, 76.20; H, 5.66; N, 3.42. Found: C, 76.16; H, 5.55; N, 2.97.

Synthesis of [1c]NiCl(PMe$_3$) (4c). Solid **2c** (74 mg, 0.08 mmol) was dissolved in THF (3 mL), and PMe_3 (0.16 mL, 1.0 M in THF, 0.16 mmol) was added at room temperature. The reaction mixture was stirred at room temperature overnight. All volatiles were removed in vacuo. The residue thus obtained was extracted with diethyl ether (6 mL), and the solution was filtered through a pad of Celite, which was further washed with diethyl ether (1 mL × 2) until the washings became colorless. The diethyl ether filtrate and washings were combined and evaporated to dryness under reduced pressure to afford the product as an emerald solid; yield 68.2 mg (89%). Emerald crystals suitable for X-ray diffraction analysis were grown from a pentane solution at −35 °C. ^{1}H NMR (C_6D_6, 500 MHz): δ 6.99 (m, 3, Ar), 6.92 (m, 1, Ar), 6.77 (t, 1, Ar), 6.25 (t, 1, Ar), 5.69 (dd, 1, Ar), 2.47 (s, 6, CH_3), 2,34 (m, 2, C*H*Me$_2$), 1.62 (dd, 6, CH*Me*$_2$), 1.34 (dd, 6, CH*Me*$_2$), 0.57 (d, 9, $^2J_{HP}$ = 8, P(C*H*$_3$)$_3$). ^{31}P{^{1}H} NMR (C_6D_6, 202.3 MHz): δ 51.1 (d, $^2J_{PP}$ = 313.5, NP), −24.24 (d, $^2J_{PP}$ = 313.5, PMe_3). ^{13}C{^{1}H} NMR (C_6D_6, 125.5 MHz): δ 168.4 (dd, J_{CP} = 26.5, 3.26, C), 153.5 (d, J_{CP} = 4.5, C), 137.4 (s, C), 133.6 (s, CH), 131.7 (s, CH), 129.6 (s, CH), 124.8 (s, CH), 113.1 (d, J_{CP} = 12.3, CH), 112.4 (d, J_{CP} = 6.0, CH), 112.4 (d, J_{CP} = 40.8, C), 25.9 (d, $^1J_{CP}$ = 26.6, CHMe$_2$), 19.6 (s, CH_3), 19.2 (d, $^2J_{CP}$ = 2.3, CH*Me*$_2$), 18.1 (s, CH*Me*$_2$), 13.2 (d, $^1J_{CP}$ = 22.8, P*Me*$_3$). Anal. Calcd for $C_{23}H_{36}ClNNiP_2$: C, 57.24; H, 7.52; N, 2.90. Found: C, 57.29; H, 7.59; N, 2.86.

General Procedures for the Synthesis of [1b,c]NiR(PMe$_3$) (R = Me (5b,c), CH$_2$SiMe$_3$ (6b,c), Ph (7b,c)). One equivalent of RMgCl was added dropwise to a solution of **4b,c** in THF at −35 °C. The reaction mixture was naturally warmed to room temperature and stirred overnight. All volatiles were removed in vacuo. The residue thus obtained was triturated with pentane to give a red or brownish red solid. Benzene was added. The benzene solution was filtered through a pad of Celite, which was further washed with benzene until the washings became colorless. The filtrate and washings were combined and evaporated to dryness under reduced pressure to afford the product as a red or brownish red crystalline solid.

Synthesis of [1c]NiMe(PMe$_3$) (5c). Ruby crystals suitable for X-ray diffraction analysis were grown from a concentrated pentane solution at −35 °C; yield 77%. **Major isomer (trans):** ^{1}H NMR (C_6D_6, 500 MHz) δ 7.14 (td, 1, Ar), 7.09 (d, 2, Ar), 6.97 (t, 1, Ar), 6.92 (t, 1, Ar), 6.34 (t, 1, Ar), 5.92 (dd, 1, Ar), 2.43 (s, 6, ArC*H*$_3$), 2.18 (m, 2, C*H*Me$_2$), 1.28 (dd, 6, CH*Me*$_2$), 1.24 (dd, 6, CH*Me*$_2$), 0.48 (dd, 9, $^2J_{HP}$ = 7.5, $^4J_{HP}$ = 1.5, P(C*H*$_3$)$_3$), −0.69 (dd, 3, $^3J_{HP}$ = 13.0 and 7.0, NiC*H*$_3$); ^{31}P{^{1}H} NMR (C_6D_6, 202.3 MHz) δ 45.5 (d, $^2J_{PP}$ = 295.7, NP), −20.0 (d, $^2J_{PP}$ = 295.7, PMe_3); ^{13}C{^{1}H} NMR (C_6D_6, 125.5 MHz) δ 167.6 (dd, J_{CP} = 26.1, J_{CP} = 4.6, C), 155.9 (dd, J_{CP} = 0.9 and 1.9, C), 136.3 (s, C), 133.1 (d, J_{CP} = 1.4, CH), 131.8 (t, J_{CP} = 1.9, CH), 129.3 (s, CH), 123.5 (s, CH), 112.7 (dd, J_{CP} = 38.0 and 1.4, C), 111.9 (d, J_{CP} = 10.9, CH), 110.8 (d, J = 5.5, CH), 24.7 (d, $^1J_{CP}$ = 24.7, CHMe$_2$), 19.7 (s, ArCH$_3$), 19.3 (d, $^2J_{CP}$ = 4.5, CH*Me*$_2$), 18.4 (d, $^2J_{CP}$ = 1.4, CH*Me*$_2$), 13.6 (dd, $^1J_{CP}$ = 21.5, $^3J_{CP}$ = 1.9, P(CH$_3$)$_3$), −18.5 (dd, $^2J_{CP}$ = 33.9 and 23.3, NiCH$_3$). **Minor isomer (cis):**[55] ^{1}H NMR (C_6D_6, 500 MHz) δ 7.33 (d, Ar), 6.40 (m, Ar), 6.09 (dd, Ar), 2.45 (s, 6, ArC*H*$_3$), 1.93 (m, 2, C*H*Me$_2$), 1.18 (dd, 6, CH*Me*$_2$), 1.07 (dd, 6, CH*Me*$_2$), 0.82 (d, 9, $^2J_{HP}$ = 8.5, P(C*H*$_3$)$_3$), −0.42 (dd, 3, $^3J_{HP}$ = 3.5 and 7.5, NiC*H*$_3$); ^{31}P{^{1}H} NMR (C_6D_6, 202.3 MHz) δ 47.7 (d, $^2J_{PP}$ = 21.7, NP), −9.1 (d, $^2J_{PP}$ = 21.7, PMe_3); ^{13}C{^{1}H} NMR (C_6D_6, 125.5 MHz) δ 136.5 (s, C), 133.4 (s, C), 132.4 (s, C), 129.8 (s, CH), 123.6 (s, CH), 113.2 (dd, J_{CP} = 10.0 and 2.3, C), 111.5 (d, J_{CP} = 5.5, C), 25.5 (d, $^1J_{CP}$ = 7.3, CHMe$_2$), 20.3 (d, $^2J_{CP}$ = 7.4, CH*Me*$_2$), 19.7 (d, $^2J_{CP}$ = 10.2, CH*Me*$_2$), 18.7 (s, ArCH$_3$), 18.0 (dd, $^1J_{CP}$ = 30.1, $^3J_{CP}$ = 3.6, (PCH$_3$)$_3$), NiMe was not found due to low signal intensity. Anal. Calcd for $C_{24}H_{39}NNiP_2$: C, 62.34; H, 8.51; N, 3.03. Found: C, 61.87; H, 8.56; N, 2.92.

Synthesis of [1b]NiCH$_2$SiMe$_3$(PMe$_3$) (6b). Red crystals suitable for X-ray diffraction analysis were grown by layering pentane on a concentrated diethyl ether solution at −35 °C; yield 88%. ^{1}H NMR (C_6D_6, 500 MHz): δ 7.85 (m, 4, Ar), 7.26 (t, 1, Ar), 7.13 (s, 4, Ar), 7.08 (m, 5, Ar), 6.88 (t, 1, Ar), 6.34 (t, 1, Ar), 6.01 (dd, 1, Ar), 3.66 (br s, 2, C*H*Me$_2$), 1.13 (m, 6, CH*Me*$_2$), 1.06 (m, 6, CH*Me*$_2$), 0.62 (d, 9, $^2J_{HP}$ = 7.5, PMe_3), 0.14 (s, 9, NiCH$_2$Si*Me*$_3$), −0.70 (br s, 2, NiC*H*$_2$SiMe$_3$). ^{31}P{^{1}H} NMR (C_6D_6, 202.3 MHz): δ 34.4 (d, $^2J_{PP}$ = 318.3, NP), −22.5 (d, $^2J_{PP}$ = 317.5, PMe_3). ^{13}C{^{1}H} NMR (C_6D_6, 125.5 MHz): δ 168.9 (dd, J_{CP} = 29.2 and 2.8, C), 153.8 (s, C), 145.9 (s, C), 134.5 (d, J_{CP} = 10.0, CH), 133.5 (s, CH), 133.0 (s, CH), 130.2 (d, J_{CP} = 2.3, CH), 128.6 (d, J_{CP} = 13.3, CH), 124.9 (s, CH), 124.7 (s, CH), 116.3 (d, J_{CP} = 11.8, CH), 112.9 (d, J_{CP} = 1.9, C), 112.5 (d, J_{CP} = 1.4, C), 112.3 (d, J_{CP} = 6.4, CH), 25.3 (s, CH*Me*$_2$), 24.0 (s, CH*Me*$_2$), 15.0 (dd, J_{CP} = 21.5 and 1.8, P*Me*$_3$), 3.9 (s, CH$_2$Si(CH$_3$)$_3$), −13.4 (dd, $^2J_{CP}$ = 18.2 and 25.2, NiCH$_2$Si(CH$_3$)$_3$). After multiple attempts even with X-ray-quality crystals, we were not able to obtain satisfactory analysis data for this compound. Anal. Calcd for $C_{37}H_{51}NNiP_2Si$: C, 67.47; H, 7.81; N, 2.13. Found: C, 67.75; H, 7.50; N, 1.35.

Synthesis of [1c]NiCH$_2$SiMe$_3$(PMe$_3$) (6c). Red crystals suitable for X-ray diffraction analysis were grown from a concentrated pentane solution at −35 °C; yield 75%. ^{1}H NMR (C_6D_6, 500 MHz): δ 7.13 (t, 1, Ar), 7.07 (d, 1, Ar), 6.93 (t, 1, Ar), 6.90 (t, 1, Ar), 6.32 (t, 1, Ar), 5.84 (dd, 1, Ar), 2.51 (s, 6, ArC*H*$_3$), 2.25 (m, 2, C*H*Me$_2$), 1.28 (dd, 6, CH*Me*$_2$), 1.25 (dd, 6, CH*Me*$_2$), 0.58 (d, 9, $^2J_{HP}$ = 7.5, P(C*H*$_3$)$_3$), 0.27 (s, 9, CH$_2$Si*Me*$_3$), −0.93 (dd, 2, $^3J_{HP}$ = 10.5 and 15.5, NiC*H*$_2$SiMe$_3$). ^{31}P{^{1}H} NMR (C_6D_6, 202.3 MHz): δ 42.9 (d, $^2J_{PP}$ = 305.4, NP), −26.3 (d, $^2J_{PP}$ = 305.4, PMe_3). ^{13}C{^{1}H} NMR (C_6D_6, 125.5 MHz): δ 166.8 (dd, J_{CP} = 24.7 and 4.5, C), 154.8 (s, C), 136.5 (s, C), 132.7 (s, CH), 131.0 (s, CH), 129.3 (s, CH), 123.5 (s, CH), 113.6 (d, J_{CP} = 38.4, C), 112.9 (d, J = 11.0, CH), 110.8 (d, J = 5.5, CH), 24.4 (d, $^1J_{CP}$ = 23.9, CHMe$_2$), 20.6 (s, CH*Me*$_2$), 20.1 (d, $^2J_{CP}$ = 3.6, CH*Me*$_2$), 18.7 (s, ArCH$_3$), 15.1 (dd, $^1J_{CP}$ = 19.2, $^3J_{CP}$ = 1.9, P(CH$_3$)$_3$), 4.2 (s, Si*Me*$_3$), −18.9 (dd, $^2J_{CP}$ = 17.4 and 30.2, NiCH$_2$). Anal. Calcd for $C_{27}H_{47}NNiP_2Si$: C, 60.67; H, 8.87; N, 2.62. Found: C, 60.52; H, 8.93; N, 2.52.

Synthesis of [1c]NiPh(PMe$_3$) (7c). Brownish red crystals suitable for X-ray diffraction analysis were grown from a concentrated diethyl ether solution at −35 °C; yield 83%. ^{1}H NMR (C_6D_6, 500 MHz): δ 7.45 (d, 2, Ar), 7.13 (d, 2, Ar), 7.04 (t, 1, Ar), 7.00 (t, 1, Ar), 6.93 (t, 3, Ar), 6.85 (t, 1, Ar), 6.36 (t, 1, Ar), 5.93 (dd, 1, Ar), 2.50 (s, 6, ArC*H*$_3$), 2.31 (m, 2, C*H*Me$_2$), 1.12 (dd, 6, CH*Me*$_2$), 0.95 (dd, 6, CH*Me*$_2$), 0.23 (d, 9, $^2J_{HP}$ = 8.0, P(C*H*$_3$)$_3$). ^{31}P{^{1}H} NMR (C_6D_6, 202.3 MHz): δ 40.6 (d, $^2J_{PP}$ = 278.0, NP), −24.3 (d, $^2J_{PP}$ = 278.0, PMe_3). ^{13}C{^{1}H} NMR (C_6D_6, 125.5 MHz): δ 167.8 (dd, J_{CP} = 25.6 and 4.1, C), 155.4 (s, C), 150.9 (dd, J_{CP} = 33.9 and 40.8, C), 139.2 (t, J_{CP} = 4.1, CH), 136.6 (s, C), 133.3 (d, J_{CP} = 1.4, CH), 131.9 (t, J_{CP} = 1.8, CH), 129.5 (s, CH), 126.5 (t, J_{CP} = 3.1, CH), 123.8 (s, CH), 122.5 (t, J_{CP} = 2.8, CH), 112.0 (d, J_{CP} = 8.5, CH), 111.8 (d, J_{CP} = 37.4, C), 111.4 (d, J = 5.5, CH), 23.6 (d, $^1J_{CP}$ = 26.5, CHMe$_2$), 19.6 (s, Ar*Me*), 18.0 (d, $^2J_{CP}$ = 3.6, CH*Me*$_2$), 17.3 (s, CH*Me*$_2$), 13.7 (dd, $^1J_{CP}$ = 23.9, $^3J_{CP}$ = 1.4, P(CH$_3$)$_3$). Anal. Calcd for $C_{29}H_{41}NNiP_2$: C, 66.42; H, 7.89; N, 2.67. Found: C, 66.14; H, 7.90; N, 2.53.

Synthesis of [1c]NiH(PMe$_3$) (8c). *Method 1.* Solid **4c** (50 mg, 0.10 mmol) was dissolved in THF (4 mL) and cooled to −35 °C. To

dx.doi.org/10.1021/om5006353 | *Organometallics* XXXX, XXX, XXX−XXX

this was added $LiHBEt_3$ (0.10 mL, 1 M in THF, 0.10 mmol) dropwise. The reaction mixture was naturally warmed to room temperature and stirred overnight. All volatiles were removed in vacuo. The brown residue thus obtained was triturated with pentane (2 mL × 2), and diethyl ether (8 mL) was added. The diethyl ether solution was filtered through a pad of Celite, which was further washed with diethyl ether (1 mL × 2) until the washings became colorless. The diethyl ether filtrate and washings were combined and evaporated to dryness under reduced pressure to afford the product as a red solid. Red crystals suitable for X-ray diffraction analysis were grown from a concentrated diethyl ether solution at −35 °C; yield 37.9 mg (82%).

Method 2. Experiments were conducted with procedures similar to those of method 1, except that 1 equiv of EtMgCl or *n*BuMgCl was used in place of $LiHBEt_3$, leading to the formation of **8c** quantitatively. ^{1}H NMR (C_6D_6, 500 MHz): δ 7.14 (s, 2, Ar), 7.09 (td, 1, Ar), 6.99 (m, 1, Ar), 6.97 (tt, 1, Ar), 6.37 (t, 1, Ar), 6.04 (dd, 1, Ar), 2.40 (s, 6, ArCH_3), 2.08 (m, 2, CHMe$_2$), 1.27 (dd, 6, CHMe_2), 1.14 (dd, 6, CHMe_2), 0.59 (dd, 9, $^2J_{HP}$ = 8.0, $^4J_{HP}$ = 1.5, P(CH_3)$_3$), −20.24 (dd, 1, $^2J_{HP}$ = 72.5 and 82.0, NiH). ^{31}P{^{1}H} NMR (C_6D_6, 202.3 MHz): δ 63.3 (d, $^2J_{PP}$ = 262.6, NP), −19.9 (d, $^2J_{PP}$ = 262.6, PMe$_3$). ^{13}C{^{1}H} NMR (C_6D_6, 125.5 MHz): δ 168.4 (dd, J_{CP} = 27.0 and 4.1, C), 155.3 (d, J_{CP} = 1.9, C), 135.7 (s, C), 133.6 (d, J_{CP} = 1.4, CH), 132.1 (t, J_{CP} = 1.9, CH), 129.1 (s, CH), 123.3 (s, CH), 113.6 (d, J_{CP} = 34.8, C), 111.4 (d, J_{CP} = 11.9, CH), 111.1 (d, J_{CP} = 5.4, CH), 25.1 (dd, J_{CP} = 29.2 and 1.8, CHMe$_2$), 20.2 (d, J_{CP} = 5.5, CHMe_2), 19.4 (s, ArCH_3), 18.7 (d, J_{CP} = 1.0, CHMe_2), 17.0 (dd, $^1J_{CP}$ = 24.7, $^3J_{CP}$ = 2.3, P(CH_3)$_3$). Anal. Calcd for $C_{23}H_{37}NNiP_2$: C, 61.62; H, 8.33; N, 3.13. Found: C, 61.36; H, 8.42; N, 3.00.

General Procedures for Catalytic Kumada Couplings. A vial was sequentially charged with **2** (1.0 mg for each single experiment, corresponding to 0.5 mol %), THF (2 mL), Grignard reagent (1.1 equiv), phenyl halide (1.0 equiv), and a magnetic stir bar. The solution was stirred at the prescribed temperature in a temperature-controlled bath for 12 h and quenched with deionized water. The products were extracted with diethyl ether. The diethyl ether solution was separated from the aqueous layer, dried over $MgSO_4$, and filtered through a short Al_2O_3 column prior to GC or GC/MS analysis.

■ ASSOCIATED CONTENT

Ⓢ Supporting Information

Tables, a figure, and CIF files giving X-ray crystallographic data for **2d**, **3a**, **4c**, **5c**, **6b**,**c**, **7c**, and **8c** (CCDC reference numbers 999526−999533). This material is available free of charge via the Internet at http://pubs.acs.org.

■ AUTHOR INFORMATION

Corresponding Author

*E-mail for L.-C.L.: lcliang@mail.nsysu.edu.tw.

Author Contributions

§These authors contributed equally to this study.

Notes

The authors declare no competing financial interest.

■ ACKNOWLEDGMENTS

We thank the Ministry of Science and Technology of Taiwan for financial support (NSC 99-2113-M-110-003-MY3 and NSC 102-2113-M-110-002-MY3), Mr. Ting-Shen Kuo (NTNU) for assistance with X-ray crystallography, and the National Center for High-performance Computing (NCHC) for the access to chemical databases. M.-T.C. thanks the Ministry of Science and Technology for a postdoctoral fellowship (NSC 102-2811-M-110-009).

■ REFERENCES

(1) Johansson Seechurn, C. C. C.; Kitching, M. O.; Colacot, T. J.; Snieckus, V. *Angew. Chem., Int. Ed.* **2012**, *51*, 5062−5085.

(2) de Mejeire, A.; Diederich, F. *Metal-Catalyzed Cross-Coupling Reactions*, 2nd ed.; Wiley-VCH: Weinheim, Germany, 2004.

(3) Tamao, K.; Sumitani, K.; Kumada, M. *J. Am. Chem. Soc.* **1972**, *94*, 4374−4376.

(4) Corriu, R. J. P.; Masse, J. P. *J. Chem. Soc., Chem. Commun.* **1972**, 144a−144a.

(5) Knappke, C. E. I.; Jacobi von Wangelin, A. *Chem. Soc. Rev.* **2011**, *40*, 4948−4962.

(6) Crabtree, R. H. *The Organometallic Chemistry of the Transition Metals*, 4th ed.; Wiley-Interscience: Hoboken, NJ, 2005.

(7) Collman, J. P.; Hegedus, L. S.; Norton, J. R.; Finke, R. G. *Principles and Applications of Organotransition Metal Chemistry*; University Science Books: Mill Valley, CA, 1987.

(8) Breitenfeld, J.; Ruiz, J.; Wodrich, M. D.; Hu, X. L. *J. Am. Chem. Soc.* **2013**, *135*, 12004−12012.

(9) Ren, P.; Vechorkin, O.; von Allmen, K.; Scopelliti, R.; Hu, X. L. *J. Am. Chem. Soc.* **2011**, *133*, 7084−7095.

(10) Guisan-Ceinos, M.; Tato, F.; Bunuel, E.; Calle, P.; Cardenas, D. J. *Chem. Sci.* **2013**, *4*, 1098−1104.

(11) Iwasaki, T.; Takagawa, H.; Singh, S. P.; Kuniyasu, H.; Kambe, N. *J. Am. Chem. Soc.* **2013**, *135*, 9604−9607.

(12) Yorimitsu, H.; Oshima, K. *Pure Appl. Chem.* **2006**, *78*, 441−449.

(13) Sherry, B. D.; Fürstner, A. *Acc. Chem. Res.* **2008**, *41*, 1500−1511.

(14) Bedford, R. B.; Bruce, D. W.; Frost, R. M.; Hird, M. *Chem. Commun.* **2005**, 4161−4163.

(15) Nakamura, M.; Matsuo, K.; Ito, S.; Nakamura, E. *J. Am. Chem. Soc.* **2004**, *126*, 3686−3687.

(16) Nagano, T.; Hayashi, T. *Org. Lett.* **2004**, *6*, 1297−1299.

(17) Liang, L.-C. *Coord. Chem. Rev.* **2006**, *250*, 1152−1177.

(18) Liang, L.-C.; Chien, P.-S.; Huang, Y.-L. *J. Am. Chem. Soc.* **2006**, *128*, 15562−15563.

(19) Liang, L.-C.; Lin, J.-M.; Lee, W.-Y. *Chem. Commun.* **2005**, 2462−2464.

(20) Liang, L.-C.; Hung, Y.-T.; Huang, Y.-L.; Chien, P.-S.; Lee, P.-Y.; Chen, W.-C. *Organometallics* **2012**, *31*, 700−708.

(21) Lee, P.-Y.; Liang, L.-C. *Inorg. Chem.* **2009**, *48*, 5480−5487.

(22) Liang, L.-C.; Chien, P.-S.; Huang, M.-H. *Organometallics* **2005**, *24*, 353−357.

(23) Chien, P.-S.; Liang, L.-C. *Inorg. Chem.* **2005**, *44*, 5147−5151.

(24) Huang, M.-H.; Liang, L.-C. *Organometallics* **2004**, *23*, 2813−2816.

(25) Hung, Y.-T.; Chen, M.-T.; Huang, M.-H.; Kao, T.-Y.; Liu, Y.-S.; Liang, L.-C. *Inorg. Chem. Front.* **2014**, *1*, 405−413.

(26) Liang, L.-C.; Li, C.-W.; Lee, P.-Y.; Chang, C.-H.; Lee, H. M. *Dalton Trans.* **2011**, *40*, 9004−9011.

(27) Liang, L.-C.; Chien, P.-S.; Hsiao, Y.-C.; Li, C.-W.; Chang, C.-H. *J. Organomet. Chem.* **2011**, *696*, 3961−3965.

(28) Liang, L.-C.; Chien, P.-S.; Lee, P.-Y.; Lin, J.-M.; Huang, Y.-L. *Dalton Trans.* **2008**, 3320−3327.

(29) Liang, L.-C.; Chien, P.-S.; Lin, J.-M.; Huang, M.-H.; Huang, Y.-L.; Liao, J.-H. *Organometallics* **2006**, *25*, 1399−1411.

(30) Liang, L.-C.; Chien, P.-S.; Lee, P.-Y. *Organometallics* **2008**, *27*, 3082−3093.

(31) Liang, L.-C.; Lin, J.-M.; Hung, C.-H. *Organometallics* **2003**, *22*, 3007−3009.

(32) Liang, L.-C.; Lee, W.-Y.; Hung, Y.-T.; Hsiao, Y.-C.; Cheng, L.-C.; Chen, W.-C. *Dalton Trans.* **2012**, *41*, 1381−1388.

(33) Liang, L.-C.; Lee, W.-Y.; Yin, C.-C. *Organometallics* **2004**, *23*, 3538−3547.

(34) Masotti, H.; Wallet, J. C.; Peiffer, G.; Petit, F.; Mortreux, A.; Buono, G. *J. Organomet. Chem.* **1986**, *308*, 241−252.

(35) Liang, L.-C.; Lee, W.-Y.; Tsai, T.-L.; Hsu, Y.-L.; Lee, T.-Y. *Dalton Trans.* **2010**, *39*, 8748−8758.

(36) Liang, L.-C.; Huang, M.-H.; Hung, C.-H. *Inorg. Chem.* **2004**, *43*, 2166−2174.

(37) Liang, L.-C.; Lee, W.-Y.; Hung, C.-H. *Inorg. Chem.* **2003**, *42*, 5471−5473.

(38) Tran, B. L.; Pink, M.; Mindiola, D. J. *Organometallics* **2009**, *28*, 2234−2243.

(39) Note that this reaction is complete in <10 min.
(40) Yang, L.; Powell, D. R.; Houser, R. P. *Dalton Trans.* **2007**, 955−964.
(41) The metathetical reaction of **2b** with $PhCH_2MgCl$ gave [**1b**]Ni(η^3-CH_2Ph) in 94% isolated yield; see reference 33.
(42) $^{31}P\{^1H\}$ NMR (THF, 121 MHz, 25 °C): δ 40.7 (d, $^2J_{PP}$ = 285, NP), −21.8 (d, $^2J_{PP}$ = 285, PMe_3).
(43) $^{31}P\{^1H\}$ NMR (THF, 121 MHz, 25 °C): δ 41.4 (d, $^2J_{PP}$ = 289, NP), −22.1 (d, $^2J_{PP}$ = 289, PMe_3).
(44) Klein, H.-F.; Beck, R.; Hetche, O. *Eur. J. Inorg. Chem.* **2003**, *2003*, 232−239.
(45) Heinicke, J.; He, M. Z.; Dal, A.; Klein, H. F.; Hetche, O.; Keim, W.; Florke, U.; Haupt, H. J. *Eur. J. Inorg. Chem.* **2000**, 431−440.
(46) Alcock, N. W. *Adv. Inorg. Chem. Radiochem.* **1972**, *15*, 1−58.
(47) Breitenfeld, J.; Vechorkin, O.; Corminboeuf, C.; Scopelliti, R.; Hu, X. L. *Organometallics* **2010**, *29*, 3686−3689.
(48) Jana, R.; Pathak, T. P.; Sigman, M. S. *Chem. Rev.* **2011**, *111*, 1417−1492.
(49) Rosen, B. M.; Quasdorf, K. W.; Wilson, D. A.; Zhang, N.; Resmerita, A.-M.; Garg, N. K.; Percec, V. *Chem. Rev.* **2010**, *111*, 1346−1416.
(50) Terao, J.; Todo, H.; Watabe, H.; Ikumi, A.; Shinohara, Y.; Kambe, N. *Pure Appl. Chem.* **2008**, *80*, 941−951.
(51) Hatakeyama, T.; Hashimoto, S.; Ishizuka, K.; Nakamura, M. *J. Am. Chem. Soc.* **2009**, *131*, 11949−11963.
(52) Sheldrick, G. M. *SADABS*; University of Göttingen, Göttingen, Germany, 1996.
(53) Sheldrick, G. M. *SHELXTL, Version 5.1*; Bruker AXS Inc., Madison, WI, 1998.
(54) Spek, A. L. *PLATON-A Multipurpose Crystallographic Tool*; Utrecht University, The Netherlands, 2003.
(55) Complete assignment of aromatic signals is hampered due to their overlap with those of the major isomer.